10826 *Inorg. Chem.* **2009**, *48*, 10826–10836
DOI: 10.1021/ic901547f

Inorganic Chemistry
Article

Ligand-Solvent Interactions in a Highly Reduced Metal Chelate Complex: Medium Dependence of the One-Electron Reduction of the *bis*(Maleonitriledithiolato)Gold Dianion

Robert J. LeSuer*,† and William E. Geiger*

Department of Chemistry, University of Vermont, Burlington, Vermont 05405. †*Present address: Department of Chemistry and Physics, Chicago State University, 9501 S. King Dr., Chicago, IL 60628.*

Received August 4, 2009

The one-electron reduction of $[Au(mnt)_2]^{2-}$ (mnt = $[S_2C_2(CN)_2]^{2-}$, maleonitriledithiolate), $\mathbf{1}^{2-}$, stands out in the rich redox chemistry of metal-mnt complexes as a chemically reversible but electrochemically irreversible process. Although the $E_{1/2}$ value of the primary redox reaction $\mathbf{1}^{2-}/\mathbf{1}^{3-}$ is only slightly medium dependent (ca. −1.36 V to −1.53 V vs FcH in several nonaqueous solvents and supporting electrolytes), its chemical reversibility is dramatically solvent dependent. A quasi-Nernstian process was observed only in tetrahydrofuran (THF) at low supporting electrolyte concentrations. Fast reversible follow-up reactions, ascribed to formation of solvento-complexes $[Au(mnt)_2 \cdot Solv]^{3-}$, were observed through cyclic voltammetry (CV) studies in dichloromethane and acetonitrile. The specifically solvated trianion reverts to "unsolvated" $\mathbf{1}^{2-}$ when reoxidized, accounting for the overall chemical reversibility of the process. Owing to the fact that the ligands in $\mathbf{1}^{3-}$ are highly negatively charged, the strong specific solvation is likely to involve H-bonding interactions between the solvent and the sulfur atoms of the trianion. Ion-pairing interactions between $\mathbf{1}^{3-}$ and electrolyte cations were also shown to have a discernible effect on the $\mathbf{1}^{2-}/\mathbf{1}^{3-}$ couple in THF. The heterogeneous electron-transfer (ET) rate constant (k_s) for this couple was sufficiently low ($k_s = \sim 10^{-3}$ cm s^{-1}) to suggest a square-planar to quasi-tetrahedral structural rearrangement being intrinsic to the $\mathbf{1}^{2-}/\mathbf{1}^{3-}$ ET process. The $E_{1/2}$ separation between the $\mathbf{1}^{-}/\mathbf{1}^{2-}$ and $\mathbf{1}^{2-}/\mathbf{1}^{3-}$ couples (ca. 220 mV) is much smaller than any of those previously reported for metal-mnt complexes. The behavior of the gold-mnt trianion is a rare example of a ligand-based solvento-complex, which contrasts with the well-known metal-based solvento-complexes that are commonly observed between electron-deficient complexes and strong donor solvents.

Introduction

One of the most widely studied electron-transfer (ET) series in inorganic chemistry is that involving metal dithiolenes, for which there are, at least for the nickel group, four members related by three one-electron transfer processes (see eq 1, which labels a generalized dithiolate ligand as S−S).[1,2] Driven in part by the finding that the salts of some members of this series exhibit high conductivity and other desirable physical properties,[3] much effort has gone into investigating how alterations of the metal, ligand,

$$M(S-S)_2 \overset{e^-}{\rightleftharpoons} M(S-S)_2^{1-} \overset{e^-}{\rightleftharpoons} M(S-S)_2^{2-} \overset{e^-}{\rightleftharpoons} M(S-S)_2^{3-} \quad (1)$$

and metal−ligand redox state affect the molecular and electronic properties of these complexes as well as their oxo-counterparts.[4] Electrochemical studies, while an important contributor to the physical understanding and preparative development of the ET series, have seldom encountered mechanistically complex ET reactions. In fact, Nernstian (i.e., chemically and electrochemically reversible)[5] processes have generally been reported[6] or implicitly assumed based on different levels of inspection of cyclic voltammetry (CV)

*To whom correspondence should be addressed. E-mail: rlesuer@csu.edu (R.J.L.), william.geiger@uvm.edu (W.E.G.).

(1) (a) McCleverty, J. A. *Prog. Inorg. Chem.* **1968**, *10*, 49. (b) Mueller-Westerhoff, U. T.; Vance, B. In *Comprehensive Coordination Chemistry*; Wilkinson, G., Gillard, R. D., McCleverty, J., Eds.; Pergamon Press: Oxford, 1987; Vol. *2*, pp 595−631. (c) Clemenson, P. I. *Coord. Chem. Rev.* **1990**, *106*, 171. (d) Lim, B. S.; Fomitchev, D. V.; Holm, R. H. *Inorg. Chem.* **2001**, *40*, 4257. (e) Periyasamy, G.; Burton, N. A.; Hillier, I. H.; Vincent, M. A.; Disley, H.; McMaster, J.; Garner, C. D. *Farady Discuss.* **2007**, *135*, 469.

(2) An historical perspective on the pertinence of metal dithiolene redox systems to the development of organometallic electrochemistry has appeared. See: Geiger, W. E. *Organometallics* **2007**, *26*, 5738.

(3) (a) Pierpont, C. G.; Lange, C. W. *Prog. Inorg. Chem.* **1994**, *41*, 331. (b) Pierpont, C. G.; Attia, A. S. *Collect. Czech. Chem. Commun.* **2001**, *66*, 33.

(4) (a) Robertson, N.; Cronin, L. *Coord. Chem. Rev.* **2002**, *227*, 93. (b) Faulmann, C.; Cassoux, P. *Prog. Inorg. Chem.* **2004**, *52*, 399.

(5) Bard, A. J.; Faulkner, L. R. *Electrochemical Methods*, 2nd ed.; John Wiley & Sons: New York, 2001; pp 239−242.

 Published on Web 10/19/2009

Scheme 1

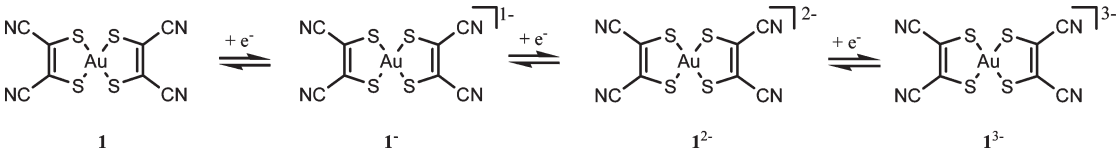

1 **1$^-$** **1^{2-}** **1^{3-}**

scans. An exception to this generality is found in gold complexes of one of the historically most important dithiolate ligands, maleonitriledithiolate, $[S_2C_2(CN)_2]^{2-}$ (mnt). Although originally prepared as the square-planar monoanion $[Au(mnt)_2]^-$,[7] it was the one-electron reduction product, $[Au(mnt)_2]^{2-}$, that became the focus of intense investigation[8,9] owing to the fact that assignment of two electrons to each mnt ligand left the gold atom in the very rare formal +2 oxidation state. The question of the electronic configuration of $[Au(mnt)_2]^{2-}$, one of the most interesting entries in the investigation of "innocent versus non-innocent" ligands,[1d,10] can now be considered solved. Both electron paramagnetic resonance (EPR) studies[9] and density functional theory (DFT) calculations[11] are in agreement that the singly occupied molecular orbital (SOMO) of $[Au(mnt)_2]^{2-}$ consists of a minor orbital contribution from the gold atom (15−25% d_{xy}) and a major ligand contribution from the four sulfur atoms (75−85% in the sulfur 3p orbitals).

We were intrigued by an aspect of the gold-mnt story that had received little attention, namely, that $[Au(mnt)_2]^{2-}$ could be further reduced[12] to form an apparent trianion at a potential that was close to that of the well-studied $[Au(mnt)_2]^{-/2-}$ couple. Although this is of some import in that it completes the four-membered[13] ET system for gold mnt (Scheme 1), the trianion would hardly be unique in either its charge (square-planar trianions of the cobalt group,[6d,e] M = Co, Rh, and nickel group,[6a−c,14] M = Ni, Pd, Pt, are well-known) or its total metal electron count (see $[Cu(mnt)_2]^{3-}$).[12] However, these other systems generally exhibited Nernstian-type $[M(mnt)_2]^{2-/3-}$ redox processes, whereas the report on the $[Au(mnt)_2]^{2-/3-}$ couple[12] placed it in the inherently interesting[15] category of a chemically reversible but *electrochemically irreversible* process. The current work therefore had its origin in the expectation that a detailed voltammetric study would be informative about general aspects of the structures, properties, and reactivities (including nucleophilic reactions[16]) of electron-rich metal dithiolenes in addition to delineating the effects responsible for the electrochemical irreversibility of the $[Au(mnt)_2]^{2-/3-}$ couple.

There was some reason to expect that $[Au(mnt)_2]^{2-}$ might follow a dissimilar ET pathway compared to its Ni group and Cu counterparts owing to the fact that its redox orbital is predominantly ligand-based,[11] whereas those of the other metals are highly metal-based (Ni,[6a−c,14] Pd,[6c,14] Pt,[6c,14] Cu[17,18]). The present paper details the dramatically different electrochemical behavior of the gold system and concludes that the $[Au(mnt)_2]^{2-/3-}$ ET process involves an AuS_4 structural rearrangement as well as changes in the sulfur-atom electron density which promote the formation of solvento complexes between $[Au(mnt)_2]^{3-}$ and strong-acceptor solvents capable of H-bonding. The effects of ion-pairing between the highly negatively charged gold-mnt trianion and the tetraalkylammonium ions of the supporting electrolyte are shown to have influence on the shapes of the voltammetric waves in some lower polarity solvents.

Experimental Section

Non-electrochemical experiments involving the $[Au(mnt)_2]^-$ complex were carried out under ambient conditions. Electrochemical experiments and chemical reductions were carried out in a Vacuum Atmospheres drybox under nitrogen.

Reagents. Tetraalkylammonium salts of $[Au(mnt)_2]^-$ were prepared using the literature method[7] and employing different tetraalkylammonium bromides in the final step. The salts were recrystallized from 1:2 acetone/isopropanol and vacuum-dried. The tetraalkylammonium salts of $[B(C_6F_5)_4]^-$ (TFAB) and $[B(C_6H_3(CF_3)_2)_4]^-$ ($BArF_{24}$) were prepared by metathesis of either Li[TFAB]·Et_2O or Na[$BArF_{24}$] (both obtained from Boulder Scientific Co., Boulder, CO.) with the appropriate $[NR_4]Br$ salt in aqueous methanol and recrystallized from CH_2Cl_2/diethylether. A detailed description of the preparation and purification of $[NBu_4]$[TFAB] can be found elsewhere.[19] $[NBu_4][PF_6]$ was prepared by metathesis of $[NBu_4]I$ and $[NH_4][PF_6]$ in hot acetone and recrystallized several times from 95% ethanol. $[N(C_6H_{13})_4][ClO_4]$ was prepared by metathesis of $[N(C_6H_{13})_4]Cl$ and $NaClO_4$ in hot acetone and recrystallized from 95% ethanol. Bis(triphenylphosphoroanylidine)-ammonium (PPN) salts were metathesized from PPN chloride (Aldrich), and the appropriate water-soluble salt of the anion. Na(2.2.2) cryptands were made in situ by addition of 1 equiv of 4,7,13,16,21,24-hexaoxa-1,10-diazabicyclo[8.8.8]hexacosane (Cryptofix 222, Aldrich) with Na[$BArF_{24}$]. All supporting electrolytes were vacuum-dried at 100 °C for at least 36 h. Reagent-grade solvents were first distilled from appropriate drying agents into

(6) (a) Lingane, P. J. *Inorg. Chem.* **1970**, *9*, 1162. (b) Mines, T. E.; Geiger, W. E. *Inorg. Chem.* **1973**, *12*, 1189. (c) Geiger, W. E.; Allen, C. S.; Mines, T. E.; Senftleber, F. C. *Inorg. Chem.* **1977**, *16*, 2003. (d) Vlček, A., Jr.; Vlček, A. A. *Inorg. Chim. Acta* **1979**, *34*, L189. (e) Vlček, A., Jr.; Vlček, A. A. *Inorg. Chim. Acta* **1980**, *41*, 123. (f) Wang, K. *Prog. Inorg. Chem.* **2004**, *52*, 267.

(7) (a) Davison, A.; Edelstein, N.; Holm, R. H.; Maki, A. H. *Inorg. Chem.* **1963**, *2*, 1227. (b) Waters, J. H.; Gray, H. B. *J. Am. Chem. Soc.* **1965**, *87*, 3534.

(8) Schlupp, R. L.; Maki, A. H. *Inorg. Chem.* **1974**, *13*, 44.

(9) (a) Kirmse, R.; Kampf, M.; Olk, R.-M.; Hildebrand, M.; Krautscheid, H. *Z. Anorg. Allg. Chem.* **2004**, *630*, 1433. (b) Ihlo, L.; Strösser, R.; Hofbauer, W.; Böttcher, R.; Kirmse, R. *Z. Naturforsch.* **1999**, *54b*, 597. (c) Ihlo, L.; Böttcher, R.; Olk, R.-M.; Kirmse, R. *Inorg. Chim. Acta* **1998**, *281*, 160.

(10) Periyasamy, G.; Burton, N. A.; Hillier, I. H.; Vincent, M. A.; Disley, H.; McMaster, J.; Garner, C. D. *Faraday Discuss.* **2007**, *135*, 469.

(11) Kokatam, S.-L.; Ray, K.; Pap, J.; Bill, E.; Geiger, W. E.; LeSuer, R. J.; Rieger, P. H.; Weyhermüller, T.; Neese, F.; Wieghardt, K. *Inorg. Chem.* **2007**, *46*, 1100.

(12) Best, S. P.; Ciniawsky, S. A.; Clark, R. J. H.; McQueen, R. C. S. *J. Chem. Soc., Dalton Trans.* **1993**, 2267. The cathodic voltammetry of the $[Au(mnt)_2]^{1-/2-/3-}$ couples reported in this paper was consistent with unpublished observations made previously at the University of Vermont by A. Bijunas and one of the present authors.

(13) A fifth (monocationic) member of the gold dithiolene series has been isolated using a (di-*tert*-butylphenyl)ethylene-dithiolate ligand in place of mnt. See reference 11.

(14) Senftleber, F. C.; Geiger, W. E. *J. Am. Chem. Soc.* **1975**, *97*, 5018.

(15) Chemically reversible but electrochemically irreversible ET processes may be generally traced to either a slow ET step (possibly involving a significant structural change), to a reversible coupled chemical reaction, or both.

(16) Vlček, A. A. *Inorg. Chim. Acta* **1980**, *43*, 35.

(17) Maki, A. H.; Edelstein, N.; Davison, A.; Holm, R. H. *J. Am. Chem. Soc.* **1964**, *86*, 4580.

(18) Záliš, S.; Vlček, A. A. *Inorg. Chim. Acta* **1982**, *58*, 89.

(19) LeSuer, R. J.; Buttolph, C.; Geiger, W. E. *Anal. Chem.* **2004**, *76*, 6395.

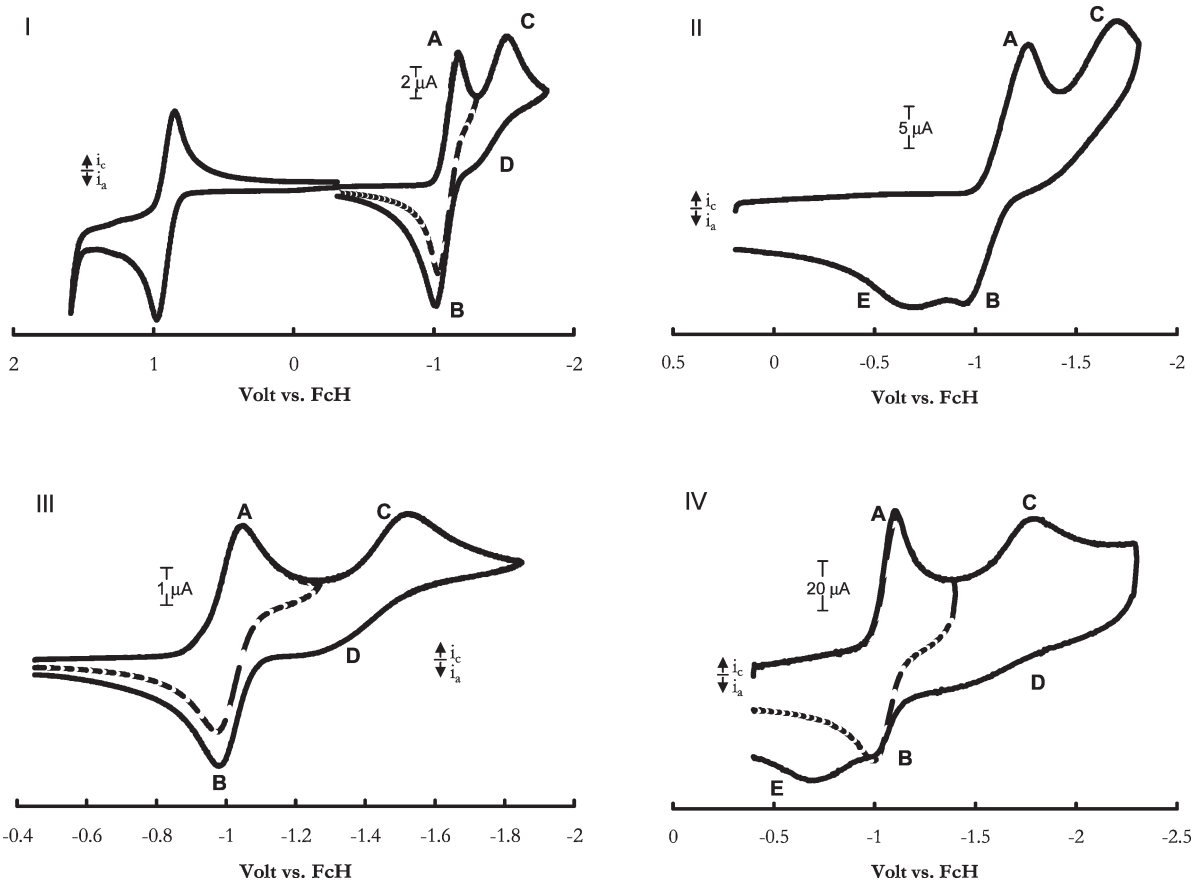

Figure 1. Survey of cyclic voltammograms. (I) 1.0 mM $\mathbf{1}^-$ in CH_2Cl_2/0.1 M[NBu_4][TFAB] at 1.5 mm GC electrode. Scan rate is 0.2 V/s. (II) Same conditions as (I) with scan rate of 3 V/s. (III) 1.2 mM $\mathbf{1}^-$ in MeCN/0.1 M [NBu_4][PF_6] at a 1 mm GC electrode. Scan rate is 0.2 V/s. (IV) Same conditions as (III) with scan rate of 80 V/s. Note that (I) depicts both oxidation and reduction waves whereas the remaining CVs cover just the reductive region.

round-bottom storage flasks that contained either CaH_2 (for dichloromethane and acetonitrile) or potassium/benzophenone (tetrahydrofuran (THF) and diethylether). If being used in an electrochemical experiment or a chemical reduction, the solvent was transferred to another vessel under static vacuum following three freeze−pump−thaw cycles and then introduced into the drybox.

Chemical Reduction of $[Au(mnt)_2]^-$. In a drybox under nitrogen, the gold-mnt dianion $[Na(2.2.2)]_2[Au(mnt)_2]$ was obtained by the treatment of 10 mg of $[NEt_4][Au(mnt)_2]$ in THF with 1 equiv of $Na[BH_4]$. When the (2.2.2) cryptand was added to the solution, the desired green salt was obtained. The gold-mnt trianion was obtained by slow addition of a THF solution of 2 equiv of decamethylcobaltocene (Aldrich) to a stirred THF solution containing 10 mg of $[NEt_4][Au(mnt)_2]$. A fine orange precipitate was formed which finally yielded an orange oily film when an excess of $[NEt_4][PF_6]$ was added. Attempts to purify the oil for chemical analysis were unsuccessful. Spectral and electrochemical characterization are discussed below.

Electrochemistry. Voltammetry and electrolysis experiments were carried out using a standard three-electrode setup controlled by a PAR 273A potentiostat with m270 PAR software. Data were then manipulated using Microsoft Excel. Voltammetry scans were recorded using a glassy carbon working electrode disk of either 1 mm or 1.5 mm diameter (Bioanalytical Systems). The electrodes were pretreated using a standard sequence of polishing with diamond paste (Buehler) of decreasing sizes (1 to 0.25 μm), interspersed by washings with deionized (18 MOhm cm^{-1}) water. The polished electrode was then dried under vacuum. For quantitative experiments in which diagnostic criteria or digital simulations were to be used for analysis, the working electrode was repolished after every scan. Although the $[Au(mnt)_2]^-$ system also behaved well at Pt electrodes, there was greater evidence of slow charge-transfer processes when using the latter. The working electrode for bulk electrolyses was made of basket-shaped platinum gauze. All potentials in this paper are referred to the ferrocene/ferrocenium reference couple[20] by the in situ method, wherein ferrocene (FcH) is added at an appropriate time in the experiment. The experimental reference electrode was a AgCl-coated silver wire, separated from solution by a fine frit. Digital simulations were performed using Digisim 3.0 (Bioanalytical Systems) and cyclic voltammetry data were obtained with the aid of positive feedback compensation of resistive loss and background subtraction. The PAR 273A potentiostat has a compliance voltage of 100 V, which was necessary for obtaining good-quality voltammograms at high scan rates in the low-polarity solvents used in this study. The compliance voltage allows the potentiostat to appropriately account for solution resistance under high (microamps) current conditions. Quasi-steady state voltammetry scans were obtained by slow scans (1 to 5 mV/s) at 1 mm electrodes and confirmed as being close to steady state by observation of scan-rate independent plateau currents.

Spectroscopy. IR spectroelectrochemistry experiments were obtained using an ATI-Mattson Infinity Series interfaced to a computer using Winfirst software. UV−vis-NIR spectra were obtained with an OLIS-converted Cary 14 spectrometer.

Results

I. Survey of Gold-mnt Voltammetry. The neutral $Au(mnt)_2$ complex is referred to as compound **1** in our discussion. Figure 1(I) displays a cyclic voltammogram

(20) (a) Gritzner, G.; Kuta, J. *Pure Appl. Chem.* **1984**, *56*, 461. (b) Connelly, N. G.; Geiger, W. E. *Chem. Rev.* **1996**, *96*, 877.

Table 1. Potentials versus Ferrocene of Reductions of $[Au(mnt)_2]^-$, $\mathbf{1}^-$, in Solvents Containing 0.10 M $[NBu_4][PF_6]$ as Supporting Electrolyte[a]

solvent	$\mathbf{1}^-/\mathbf{1}^{2-}$ ($E_{1/2}^{1,2}$)	$\mathbf{1}^{2-}/\mathbf{1}^{3-}$ ($E_{1/2}^{2,3}$)
acetonitrile	−1.00 V	−1.53 V[a]
dichloromethane	−1.11 V	−1.52 V[a]
THF	−1.14 V	−1.51 V

[a] Irreversible cathodic wave; E_{pc} at scan rate of 0.2 V s^{-1} given.

for the $[NBu_4]^+$ salt of $\mathbf{1}^-$ in dichloromethane/0.1 M $[NBu_4][PF_6]$, encompassing a potential range sufficient to include all three of the ET reactions of Scheme 1. The reversible oxidation of $\mathbf{1}^-$ to **1** at $E_{1/2}$ = 0.92 V versus FcH has been previously described,[11] as has the well-known[8,9] reduction of $\mathbf{1}^-$ to $\mathbf{1}^{2-}$ at $E_{1/2}$ = −1.11 V (see dashed line in Figure 1(I)). Continuation of the scan to more negative potentials displays the reduction of $\mathbf{1}^{2-}$ (E_{pc} = −1.53 V at this scan rate). It is important to notice the increased anodic current on the reverse sweep when the second cathodic wave is included in the scan. The magnitude of this increase suggests that the product of the reduction of $\mathbf{1}^{2-}$ is also oxidized on the reverse scan. As will be shown, the anodic activity in the region of about −1.5 V to −0.5 V is essential to understanding the chemical behavior of the trianion $\mathbf{1}^{3-}$.

The major findings of this study are as follows: (i) the heterogeneous ET rate of $[Au(mnt)_2]^{2-/3-}$ is low, indicating a significant rearrangement of the AuS_4 geometry in the charge-transfer process; (ii) the trianion $[Au(mnt)_2]^{3-}$ undergoes a chemically reversible reaction, apparently involving specific solvation at the sulfur atoms, with the strength of the sulfur-solvent interaction increasing in strong acceptor solvents capable of H-bonding; (iii) two-electron reoxidation of the trianion quantitatively regenerates $\mathbf{1}^-$, thereby giving an overall chemically reversible redox process; and (iv) ion-pairing of the trianion $[Au(mnt)_2]^{3-}$ with supporting electrolyte cations may have a significant influence on the electrode response. The closest approach to Nernstian behavior for the $[Au(mnt)_2]^{2-/3-}$ couple was found for slower voltammetry scans in THF solutions having low concentrations of supporting electrolyte (vide infra).

I.a. Effect of Solvent. Table 1 contains potentials recorded for the $\mathbf{1}^{-/2-}$ and $\mathbf{1}^{2-/3-}$ couples in the three most thoroughly studied solvents (experiments were also conducted in dimethylformamide and benzonitrile, in which $\mathbf{1}^-$ displayed behavior similar to that observed in acetonitrile). Figure 1 shows the CV scans of $\mathbf{1}^-$ observed in dichloromethane and acetonitrile. In both cases, the peaks labeled as A and B arise from the reversible $\mathbf{1}^{-/2-}$ couple, and peak C arises from the reduction of $\mathbf{1}^{2-}$ to $\mathbf{1}^{3-}$ (the one-electron nature of the process was confirmed by other analytical methods including bulk coulometry). Region D displayed only a flat shape indicative of a "CE"-type process[21] at slow scan rates (CVs (I) and (III) in Figure 1). At faster scan rates (entries II and IV) a new anodic peak, E, appeared. More detailed studies in media exhibiting this general type of behavior were carried out in dichloromethane and acetonitrile, which have much different dielectric constants but very similar high acceptor numbers (dichloromethane: ε = 8.9, AN = 20.4; acetonitrile: ε = 36.7, AN = 18.9).[22] The overall chemical reversibility of the anodic processes B, D, and E compared to the cathodic processes A and C was established by double-potential-step chronoamperometry[23] (Supporting Information, Figure S1). Bulk electrolysis of $\mathbf{1}^-$ in CH_2Cl_2 negative of the second reduction process (E_{appl} = −1.9 V) required slightly more than 2 F of charge and resulted in decomposition of the gold-mnt system, which was not surprising considering the reactivity of dichloromethane toward strong one-electron reductants.

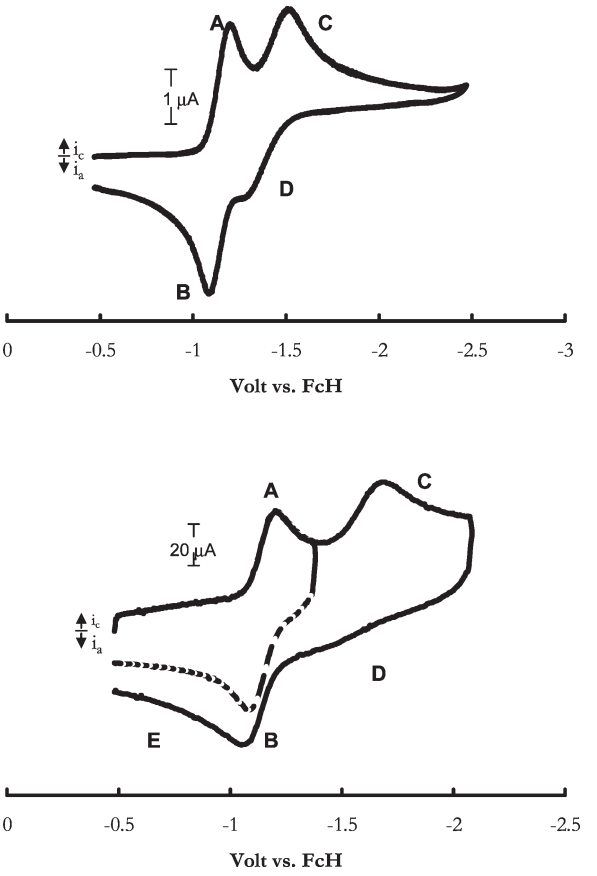

Figure 2. (Upper) 0.9 mM $\mathbf{1}^-$ in THF/0.13 M $[NBu_4][PF_6]$ at 1 mm GC electrode. Scan rate is 0.2 V/s (Lower) 0.9 mM $\mathbf{1}^-$ in THF/0.09 M $[NBu_4]$[TFAB] at 1.5 mm GC. Scan rate 80 V/s.

Figure 2 shows the CV responses for $\mathbf{1}^-$ in THF under the normal conditions of about 1 mM analyte and 100 mM supporting electrolyte.[24] The $\mathbf{1}^-/\mathbf{1}^{2-}$ couple ($E_{1/2}$ = −1.14 V) displays essentially Nernstian behavior, and standard methodologies[25] were used to calculate a lower limit for its value of k_s, the standard rate constant, as

(21) The CE mechanism is one in which a chemical reaction precedes the ET step (see reference 5, p 473). It will be shown below that the shape of this region is influenced by the rate and equilibrium constants of the reaction $[Au(mnt)_2]^{3-} \rightleftharpoons [Au(mnt)_2 \cdot Solv]^{3-}$ and the CV scan rate.

(22) Linert, W.; Fukuda, Y.; Camard, A. *Coord. Chem. Rev.* **2001**, *218*, 113.

(23) For double potential step chronoamperometry, see reference 5, pp 207−210. Using step potentials of −0.5 V to −2.0 V and a step time of 300 msec, the ratios of reverse-to-forward currents at different t/τ values reproduced those obtained for ferrocene/ferrocenium under identical conditions (e.g., 0.27 at t/τ = 2, close to the theoretical value of 0.29). See Supporting Information, Figure S1.

(24) Weakly coordinating $[B(C_6F_5)_4]^-$ was used as the electrolyte anion in the 80 V s^{-1} experiment for the purpose of lowering the solution resistance. See reference 19.

(25) It is difficult to completely eliminate the effects of solution resistance using positive feedback *iR* compensation in solvents with low dielectric constants. A lower estimate of the value of k_s was determined by ignoring the effect of uncompensated resistance and applying the Nicholson method CV scans from 0.2 V s^{-1} (ΔE_p = 70 mV) to 80 V s^{-1} (ΔE_p = 118 mV), ignoring *iR* effects. The actual k_s is likely a factor of 2 to 3 larger than the lower estimate reported here. (see: Nicholson, R. S. *Anal. Chem.* **1966**, *38*, 1406.

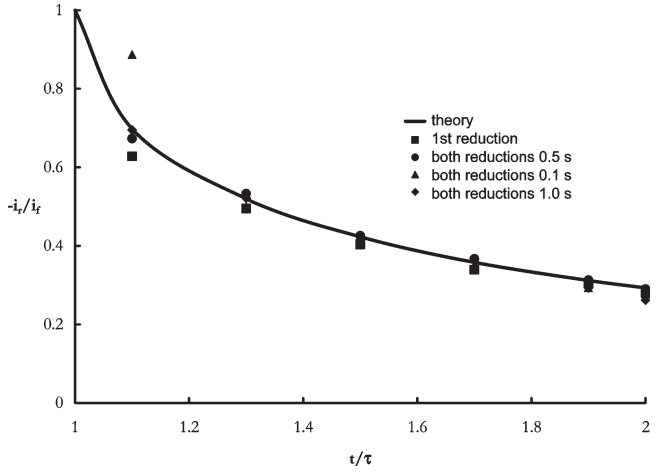

Figure 3. Double potential step chronoamperometry of $\mathbf{1}^-$ in THF with 0.1 M $[NBu_4][PF_6]$ as supporting electrolyte. The electrode was a 1 mm diameter glassy carbon disk. Step potential for the first reduction was −1.3 V vs FcH with a step time of 0.5 s. The step potential for reduction to $\mathbf{1}^{3-}$ was −1.8 V vs FcH with step times as indicated in the legend.

0.13 cm s^{-1}. The second cathodic wave, involving the reduction of $\mathbf{1}^{2-}$ to $\mathbf{1}^{3-}$, behaves as a *totally irreversible ET step* when the CV scan rates are above 1 V s^{-1}.[26] However, the second reduction was *completely chemically reversible* when the potential was reversed to the original rest potential, even though there is no new peak (E) observed in the reverse scan. This was best shown by double-potential-step chronoamperometry experiments stepping between −0.5 V and −1.8 V which agreed well with theory for a chemically reversible two-electron process going between $\mathbf{1}^-$ and $\mathbf{1}^{3-}$ (Figure 3). Voltammograms of two redox couples in close proximity, one of which exhibits slow charge transfer, may be subject to variations because of disproportionation of the one-electron intermediate. Investigation of the present system over a concentration range from 0.39 mM to 7.4 mM showed no significant voltammetric variations for scan rates varying from 0.05 V s^{-1} to 1.5 V s^{-1}, suggesting disproportionation does not play a significant role in the overall electron-transfer mechanism.

Any possibility that electrode adsorption was playing a role in the voltammetry of the $\mathbf{1}^{2-}/\mathbf{1}^{3-}$ couple was ruled out on the basis of double-potential-step-chronocoulometry, in which "Anson plots"[27] gave no evidence of specific adsorption for a 0.4 mM solution of $[NBu_4]\mathbf{1}$ in 0.09 M $[NBu_4][TFAB]$ in THF at a glassy carbon electrode when employing a 1-s step involving either one or both of the reduction processes (see Supporting Information, Figure S2).

The longer-term (about 1 h) stability of $\mathbf{1}^{3-}$ in THF was demonstrated by bulk electrolysis. Using an E_{appl} of −1.8 V for a solution of the monoanion $\mathbf{1}^-$ and allowing 1 F to pass, a green solution of the dianion $\mathbf{1}^{2-}$ was produced. Allowing the electrolysis to proceed to completion (passing a total of 2 F) produced a yellow solution of the trianion $\mathbf{1}^{3-}$ which, upon reoxidation at $E_{appl} = -0.5$ V, reproduced the original monoanion in 95% yield. By a combination of chronoamperometry and linear scan voltammetry (Supporting Information, Figure S3) of the electrolysis solutions, the diffusion coefficients, *D*, of the three differently charged complexes were determined (Table 2).

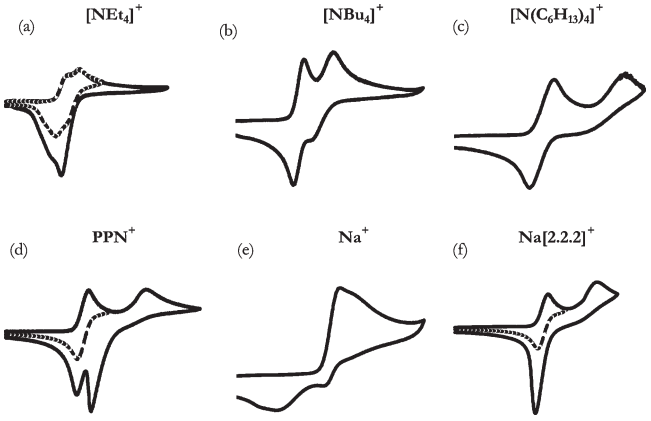

Figure 4. Cyclic voltammograms of $\mathbf{1}^-$ in the presence of various supporting electrolytes in THF. (a) $[NEt_4][TFAB]$, (b) $[NBu_4][TFAB]$, (c) $[N(C_6H_{13})_4][ClO_4]$, (d) [PPN][TFAB], (e) $Na[BArF_{24}]$, (f) [Na(2.2.2)]-$[BArF_{24}]$. Supporting electrolyte concentrations range from 0.05 to 0.1 M, and the electrode surface is glassy carbon. Scan rates were 0.2 V/s except for (e) which was 0.05 V/s.

Table 2. Diffusion Coefficients, D, Measured for Differently-Charged Ions of $[Au(mnt)_2]^{n-}$ (n = 1,2,3) in THF/0.1 M $[NBu_4][PF_6]$ at Ambient Temperature

ion	D (cm^2 s^{-1})
$[Au(mnt)_2]^-$	8.5×10^{-6}
$[Au(mnt)_2]^{2-}$	4.8×10^{-6}
$[Au(mnt)_2]^{3-}$	3.8×10^{-6}

I.b. Effect of Electrolyte. One would expect there to be significant ion-pairing interactions between the trianion $\mathbf{1}^{3-}$ and the supporting electrolyte cation in a lower polarity solvent such as THF. To discern how this effect might influence the overall ET process, a survey of the behavior of the gold-mnt/THF system in the presence of electrolyte cations was carried out. Representative results are pictured in Figure 4. An attractive feature of supporting electrolytes containing the fluorinated tetraphenylborate anion is the solubility of its salts in lower-polarity solvents, thereby opening up the possibility of conducting broad surveys of electrolyte effects such as this one. Anodic stripping peaks were observed with all but the long-chain tetraalkylammonium cations, which are presumably the least ion-pairing cations of the group. Insoluble products are clearly formed when $\mathbf{1}^{3-}$ is generated in the presence of 0.1 M $[NEt_4]^+$, PPN^+ (PPN = $[PPh_3{=}N{=}PPh_3]^+$), or $[Na(2.2.2)]^+$, and Na^+ appeared to precipitate even the dianion $\mathbf{1}^{2-}$ onto the electrode surface. Chrononocoulometry on the $[Na(2.2.2)]^+$ system confirmed adsorption of the $\mathbf{1}^{3-}$ salt on a glassy carbon electrode (Supporting Information, Figure S4). It was also clear that the potential separation of the two one-electron processes increases as the length of the alkyl chain is increased from R = ethyl to butyl to hexyl in $[NR_4]^+$. Although the complexities in the voltammetry did not allow a confident assignment of the increase in $\Delta E_{1/2}$ values ($\Delta E_{1/2} = {E_{1/2}}^{1,2} - {E_{1/2}}^{2,3}$) for $[NR_4]^+$ containing solutions, these findings are qualitatively

(26) E_{pc} for wave C undergoes a negative linear shift with log of scan rate over the range 1 to 100 V s^{-1}, with the slope of 69 mV being indicative of a charge transfer coefficient, α, of 0.43. The broadness of the wave also suggests that the α value is less than 0.5 ($E_p - E_{p/2} \approx 115$ mV; α = 0.41).

(27) Anson, F. C.; Osteryoung, R. A. *J. Chem. Educ.* **1983**, *60*, 293.

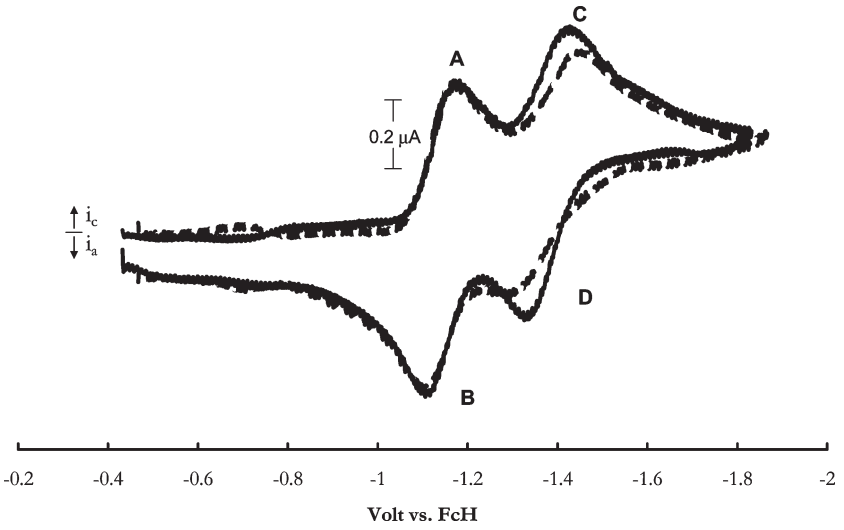

Figure 5. 0.3 mM $\mathbf{1}^-$ in THF/0.075 M [NBu_4][TFAB] (dashed line) and THF/0.008 M [NBu_4][TFAB] (solid line) at a 1.5 mm diameter glassy carbon electrode. Scan rate is 200 mV/s. Ohmic drop in both CVs partially corrected for by positive feedback compensation.

Scheme 2

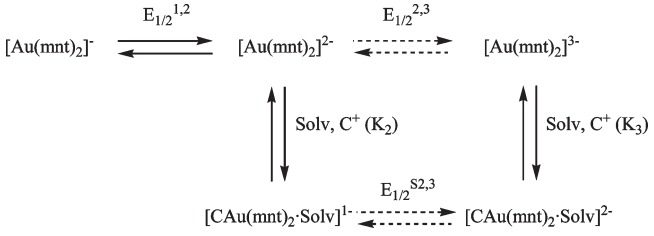

consistent with the integrated electrolyte model recently described.[28] The charge-transfer rate of the $\mathbf{1}^{2-}/\mathbf{1}^{3-}$ couple may also decrease with increasing size of the cation, as seen previously for some organic redox systems.[29]

When probing the effects of supporting electrolyte on the behavior of the gold-mnt system, an unusual result was observed in THF at low concentrations (down to 5 mM) of tetrabutylammonium-based electrolytes. As shown by the solid line in Figure 5, a decidedly more reversible-looking reduction of $\mathbf{1}^{2-}$ was observed under these conditions. A finding of this general type has been reported for the reduction of nitroalkanes and other organic compounds,[29,30] and in those cases it was clear that at higher concentrations, non-specific adsorption of the $[NBu_4]^+$ electrolyte cation on the electrode surface was retarding charge-transfer to the organic substrate. Under identical conditions, however, we found no effect of electrolyte concentration on the reversibility of the one-electron reduction of the identically charged nickel dianion, $[Ni(mnt)_2]^{2-}$ ($E_{1/2} = -2.33$ V in THF), nor was an electrolyte concentration effect seen for $\mathbf{1}^{2-}$ in dichloromethane. As detailed below, the influence of electrolyte concentration on the redox behavior of $[Au(mnt)_2]^{2-}$ can be accounted for by a combined medium effect (i.e., both solvation and ion pairing) on the $\mathbf{1}^{2-}/\mathbf{1}^{3-}$ couple in THF.

It was also noted that at low concentrations of both $[Au(mnt)_2]^-$ and $[Na(2.2.2)][BArF_{24}]$[31] (0.1 mM and 10 mM, respectively), the adsorption problems shown in Figure 4(f) were not encountered, and CV scans (Supporting Information, Figure S5) displayed a separate reversible one-electron process for $\mathbf{1}^{2-}/\mathbf{1}^{3-}$, with $k_s = 0.008$ cm s^{-1} determined by the dependence of ΔE_p on CV scan rate.

I.c. Qualitative Mechanistic Interpretation. A working hypothesis at this point was that the overall process $\mathbf{1}^{2-} \rightarrow \mathbf{1}^{3-} \rightarrow \mathbf{1}^{2-}$ involved electron-transfer steps coupled to a chemical reaction, namely, the specific solvation of the trianion (eq 3). In this model, the reduction of $\mathbf{1}^{2-}$ follows EC behavior

$$[Au(mnt)_2]^{2-} + e^- \rightleftharpoons [Au(mnt)_2]^{3-} \quad E \quad (E_{1/2}^{2,3}) \quad (2)$$

$$[Au(mnt)_2]^{3-} + Solv \rightleftharpoons [Au(mnt)_2 \cdot Solv]^{3-} \quad C \quad (3)$$

$$[Au(mnt)_2 \cdot Solv]^{3-} - e^- \rightleftharpoons [Au(mnt)_2 \cdot Solv]^{2-} \quad E \quad (E_{1/2}^{S2,3}) \quad (4)$$

(eqs 2 and 3) in which the charge-transfer reaction (eq 2) obeys quasi-reversible ET kinetics and the solvated trianion (eq 3) dominates in a strong acceptor solvent. On the reverse anodic sweep, the "desolvated" trianion $\mathbf{1}^{3-}$ is furnished too slowly for there to be appreciable anodic current near the potential $E_{1/2}^{2,3}$, following mechanistic CE behavior.[32]

The more positive anodic features observed in acetonitrile and dichloromethane (peak E in Figure 1) arise from the oxidation of $[\mathbf{1} \cdot Solv]^{3-}$ near $E_{1/2}^{S2,3}$ (eq 4). Formation of $[\mathbf{1} \cdot Solv]^{2-}$ would, of course, be followed by rapid loss of solvent to first give back $\mathbf{1}^{2-}$, which would be

(28) Barrière, F.; Geiger, W. E. *J. Am. Chem. Soc.* **2006**, *128*, 3980.
(29) (a) Evans, D. H.; Gilicinski, A. G. *J. Phys. Chem.* **1992**, *96*, 2528. (b) Petersen, R. A.; Evans, D. H. *J. Electroanal. Chem.* **1987**, *222*, 129.
(30) Fawcett, W. R.; Fedurco, M.; Opallo, M. *J. Phys. Chem.* **1992**, *96*, 9959.
(31) Na[2.2.2][$BArF_{24}$] has an electrochemical "window" from about +1.4 to −2.3 V vs Ag/AgCl in THF at a glassy carbon electrode.
(32) This voltammetric behavior places the CE process in the Saveant "KP region" (pure kinetic control), whereas the "KE region" is found in THF (intermediate kinetics). See: Savéant, J.-M. *Elements of Molecular and Biomolecular Electrochemistry*; John Wiley & Sons: New York, 2006; pp 92−94.

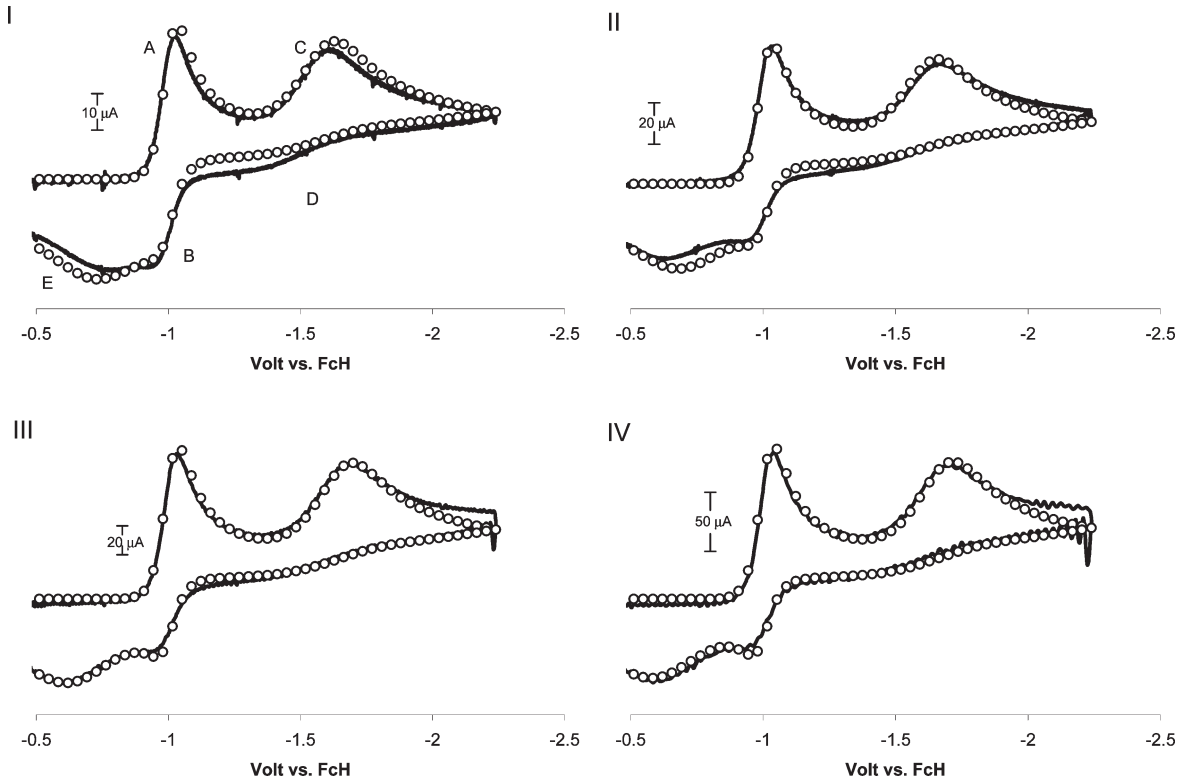

Figure 6. Simulation of $\mathbf{1}^{-}$ in MeCN at high scan rates. Circles represent simulated data. Solid lines represent experimental data at (I) 10 V/s, (II) 20 V/s, (III) 50 V/s, (IV) 80 V/s. Mechanism used to simulate voltammograms is shown in Scheme 2. Potential axis is versus ferrocene.

immediately oxidized to $\mathbf{1}^{-}$ at this potential, thus completing the chemically reversible process. Weaker solvation of $\mathbf{1}^{3-}$ by THF would allow the anodic oxidation of the unsolvated trianion to take place near $E_{1/2}{}^{2,3}$, with the flat anodic section at higher scan rates (region D in Figure 1-II and -IV) being a kinetic consequence of outrunning the rate at which desolvated $\mathbf{1}^{3-}$ is furnished on the reverse (positive-going) scan.

II. Simulation of Gold-mnt Cyclic Voltammetry. We now turn to developing an electrochemical model that adequately accounts for solvent and supporting electrolyte concentration effects on the $\mathbf{1}^{2-/3-}$ redox couple. Scheme 2 describes the overall mechanism for the two-step reduction of $\mathbf{1}^{-}$. In it, the $\mathbf{1}^{1-/2-}$ couple at $E_{1/2}{}^{1,2}$ is quasi-Nernstian, and the $\mathbf{1}^{2-/3-}$ process at $E_{1/2}{}^{2,3}$ involves a square scheme[33] in which the $\mathbf{1}^{2-}$ and $\mathbf{1}^{3-}$ ions are each subject to a general medium effect which incorporates the effects of both solvation and ion-pairing with the electrolyte cation (C^{+}). The two ET reactions in the square scheme ($E_{1/2}{}^{2,3}$ and $E_{1/2}{}^{S2,3}$) are drawn with dashed lines to emphasize that they are not Nernstian processes. Since the equilibrium constants for the coupled medium reactions are essentially the product of solvation and ion-pairing constants, the term "medium constant" is used for K_2 and K_3, which are defined in eqs 5 and 6.

$$K_2 = [\mathrm{CAu(mnt)_2 \cdot Solv^-}]/[\mathrm{Solv}][\mathrm{C^+}][\mathrm{Au(mnt)_2{}^{2-}}] \quad (5)$$

$$K_3 = [\mathrm{CAu(mnt)_2 \cdot Solv^{2-}}]/[\mathrm{Solv}][\mathrm{C^+}][\mathrm{Au(mnt)_2{}^{3-}}] \quad (6)$$

It is expected that $K_3 \gg K_2$ in both dichloromethane and THF owing to increased ion-pairing of the trianion in these lower-polarity solvents. Even though ion-pairing is weaker in acetonitrile, it should still be true that $K_3 > K_2$, owing to strong solvation of the trianion.

II.A. Simulations in Acetonitrile. When comparing the CV results in THF to those in other solvents, we chose acetonitrile over dichloromethane for the quantitative comparison to take advantage of the more accurate data available at high scan rates in acetonitrile. Figure 6 shows comparisons between experimental and simulated data in acetonitrile for CV scans between 10 V s^{-1} and 80 V s^{-1}. Considering the large number of adjustable parameters that could not be determined experimentally, we note that the optimized simulation parmeters listed in Table 3, while consistent with the CV data, may not be unique. With that caveat in mind, the most important findings were the following. The $\mathbf{1}^{2-/3-}$ couple has an $E_{1/2}$ value that is 0.25 V negative of that of the $\mathbf{1}^{-/2-}$ couple and has low values for its charge transfer coefficient ($\alpha = 0.32$) and standard ET rate constant ($k_s = 0.0012$ cm s^{-1}). The reaction of the medium (presumably dominated by solvation) with the trianion, which proceeds with a rate constant (k_f) of 3800 M^{-1} s^{-1},[34] lies strongly in favor of the solvated form ($K_3 = 440$ M^{-1}). The $E_{1/2}$ potentials and K_3 value fix the value of K_2 at 1.8×10^{-3} M^{-1}. Although some increase in ion-pairing is expected for $\mathbf{1}^{3-}$ compared to $\mathbf{1}^{2-}$, the high K_3/K_2 ratio of 2.5×10^5 is largely reflective of the much stronger solvation of the trianion.

II.B. Simulations in THF. Since the modest solvation and increased ion-pairing interactions in THF provide for

(33) Evans, D. H.; O'Connell, K. M. In *Electroanalytical Chemistry*; Bard, A. J., Ed; Marcel Dekker: New York, 1986; Vol. *14*, pp 113−208.

(34) The concentrations employed in the simulations were those of the neat solvent (acetonitrile) or the neat solvent modified by the electrolyte effect (THF, see text). Although units of M^{-1} are used here, it is to be understood that K_3 is dimensionless when the concentration of electrolyte is taken into account. The same concept is relevant to the units of k_f.

Table 3. Relevant Simulation Parameters for 1 mM $\mathbf{1}^-$ in Acetonitrile/0.1 M $[NBu_4][PF_6]$ Recorded at 2 mm gce[a]

Rxn or symbol	$E_{1/2}$ (V)	α	k_s (cm s^{-1})	K_m (M^{-1})[34]	k_f (M^{-1} s^{-1})[34]
$\mathbf{1}^{1-/2-}$ ($E_{1/2}^{1,2}$)	−1.00	0.50	1.0		
$\mathbf{1}^{2-/3-}$ ($E_{1/2}^{2,3}$)	−1.25	0.32	0.0012		
$E_{1/2}^{S2,3}$	−0.87	0.78	0.007		
K_2				0.0018	1
K_3				440	3800

[a] Symbols are defined in Scheme 2. Potentials vs ferrocene.

discernible competition between the two different medium effects, a more extensive set of 24 simulations was undertaken on data recorded in this solvent. Cyclic voltammograms of $\mathbf{1}^-$ in THF are highly dependent on the supporting electrolyte concentration. On the basis that the concentrations of the medium-rich species $[CAu(mnt)_2 \cdot Solv^{n-}]$ (n = 1 or 2) are proportional to K_m[Solv][C] (m = 2 or 3, eqs 5 and 6), the electrolyte effect was mimicked in the simulations by employing a bimolecular, reversible chemical reaction coupled to electrochemical generation of $\mathbf{1}^{3-}$. Simulations were obtained for solutions containing 8 to 75 mM supporting electrolyte and scan rates from 0.2 to 1 V/s. As noted above, CVs in THF did not exhibit effects arising from the disporportionation reaction: $2\ \mathbf{1}^{2-} \rightleftharpoons \mathbf{1}^- + \mathbf{1}^{3-}$. Nevertheless, the experimental concentration of $\mathbf{1}^-$ was kept low enough (0.28 mM) to allow pseudo-first order kinetics to apply to the coupled reactions. Some variations of diffusion coefficients (D) were necessary with changes in electrolyte concentration to obtain fits with the experimental currents measured, but the values always followed the trend $D(\mathbf{1}^-) > D(\mathbf{1}^{2-}) > D(\mathbf{1}^{3-})$, as determined experimentally. The $[B(C_6F_5)_4]^-$ salt of the tetrabutylammonium ion was employed to minimize ohmic errors.[19]

Comparison of theory with experiment was highly satisfactory over almost an order of magnitude in both electrolyte concentrations and CV scan rates. Figure 7 gives a representative grouping, and the complete set of simulations is available in Supporting Information, Figure S6. Tabulation of the most important parameters is provided in Table 4.

The chief consequence of the simulations is that they confirm the appropriateness of Scheme 2 in describing the voltammetric behavior. They show that (i) the separation of $E_{1/2}$ values for the $\mathbf{1}^{1-/2-}$ and $\mathbf{1}^{2-/3-}$ couples is changed little in THF (220 mV) compared to acetonitrile (250 mV); (ii) the slow charge-transfer and low α values of the $\mathbf{1}^{2-/3-}$ couple is confirmed; and (iii) by comparison of the K_3 values, the equilibrated form of the "medium-rich trianion", namely $[CAu(mnt)_2 \cdot Solv]^{2-}$, is destabilized by about 3 orders of magnitude in THF/$[NBu_4]^+$ compared to acetonitrile/$[NBu_4]^+$.

III. Spectroscopic Characterization of $[Au(mnt)_2]^{3-}$. The IR spectrum of $\mathbf{1}^{3-}$ generated by spectroelectrochemistry in dichloromethane/$[NBu_4][BF_4]$ has been reported (Table 5).[12] IR spectra of the three oxidation states $\mathbf{1}^-$, $\mathbf{1}^{2-}$, and $\mathbf{1}^{3-}$ were obtained in THF/$[NBu_4][PF_6]$ ex-situ by extracting samples generated by bulk electrolysis (Figure 8). As expected, absorption bands in the ν_{CN} region decrease as the negative charge on $[Au(mnt)_2]^{n-}$ increases, from 2216 cm^{-1} for n = 1 (average of two bands), to 2193 cm^{-1} for n = 2 (major band only), to 2185 cm^{-1} for n = 3 (average of major peak and shoulder). The higher-energy shoulder measured for $\mathbf{1}^{3-}$ is not likely to arise from residual $\mathbf{1}^{2-}$ owing to the fact that a linear scan voltammogram of the electrolysis solution demonstrated that the gold complex was completely reduced when the spectrum of the trianion was recorded. IR spectra of the chemically reduced complexes (see Experimental Section) were obtained as KBr pellets prepared under an inert atmosphere and are consistent with the spectra obtained on samples generated electrochemically in THF.

Electronic spectra of $\mathbf{1}^{n-}$ (n = 1, 2, 3) were measured in the region from 200 to 1100 nm and compared to the series of isoelectronic analogues, $[M(mnt)_2]^{2-}$ (M = Ni, Cu, Zn). Visible and near IR spectra of $\mathbf{1}^{2-}$ and $\mathbf{1}^{3-}$ were obtained by quantitative electrochemical reduction of 2 mM solutions of $\mathbf{1}^-$. Major features of the visible and near IR spectra are given in Table 6. Oxidation-state-independent features were seen at 1020 and 970 nm. The visible band at 745 nm for $\mathbf{1}^-$ and 720 nm for $\mathbf{1}^{2-}$ is absent for $\mathbf{1}^{3-}$ and possibly arises from a d-d transition which would be absent in the d^{10} complex, $\mathbf{1}^{3-}$.

The submillimolar concentrations needed for measuring the UV spectra of gold-mnt complexes precluded the use of electrochemistry to generate the $\mathbf{1}^{2-}$ and $\mathbf{1}^{3-}$ species. Thus, nominally 0.1 mM solutions of $\mathbf{1}^{2-}$ and $\mathbf{1}^{3-}$ were generated by chemical reduction with decamethylcobaltacene. A comparison between the gold-mnt complexes and their isoelectronic analogues is given in Supporting Information, Figure S7.

Isoelectronic species display similar numbers and shapes of features, with the major differences being in the energy of the absorptions. The structure of $[Zn(mnt)_2]^{2-}$ is known to be tetrahedral[35] and the similarities between its spectra (λ = 270 and 380 nm with two high energy shoulders) and that of $\mathbf{1}^{3-}$ (λ = 265 and 410 nm with two high energy shoulders) suggest that the structural change upon reduction of $\mathbf{1}^{2-}$ is a square-planar to tetrahedral distortion. The optical spectrum of $\mathbf{1}^{3-}$ is consistent with that of a d^{10} Au(I) configuration,[36] and the congeneric silver complex, $[Ag(mnt)_2]^{3-}$ (as the $[K(2.2.2)]_3$ salt), has been shown by X-ray crystallography[37] to be tetrahedral.

Discussion

From the starting point of the monoanion of this series, $[Au(mnt)_2]^-$ is reduced in two consecutive and thermodynamically closely spaced one-electron processes. The second of these reactions, involving the $[Au(mnt)_2]^{2-/3-}$ couple, exhibits a charge-transfer rate than appears to be slower than any reported or implied in the significant previous literature of metal-mnt redox chemistry. A structure change from square-planar[9a] $[Au(mnt)_2]^{2-}$ to a tetrahedral or distorted tetrahedral configuration for $[Au(mnt)_2]^{3-}$ is likely to be responsible for the increased reorganization energy for this

(35) Holm, R. H.; O'Connor, M. J. *Prog. Inorg. Chem.* **1971**, *14*, 241.
(36) The dianions $[M(mnt)_2]^{2-}$ generally show intense optical absorption (see ref 1a, pp 114−116). An exception is the d^{10} zinc complex, which we find to be optically silent in the 400−800 nm region (see Supporting Information, Figure S7).
(37) McLauchlan, C. C.; Ibers, J. A. *Inorg. Chem.* **2001**, *40*, 1809.

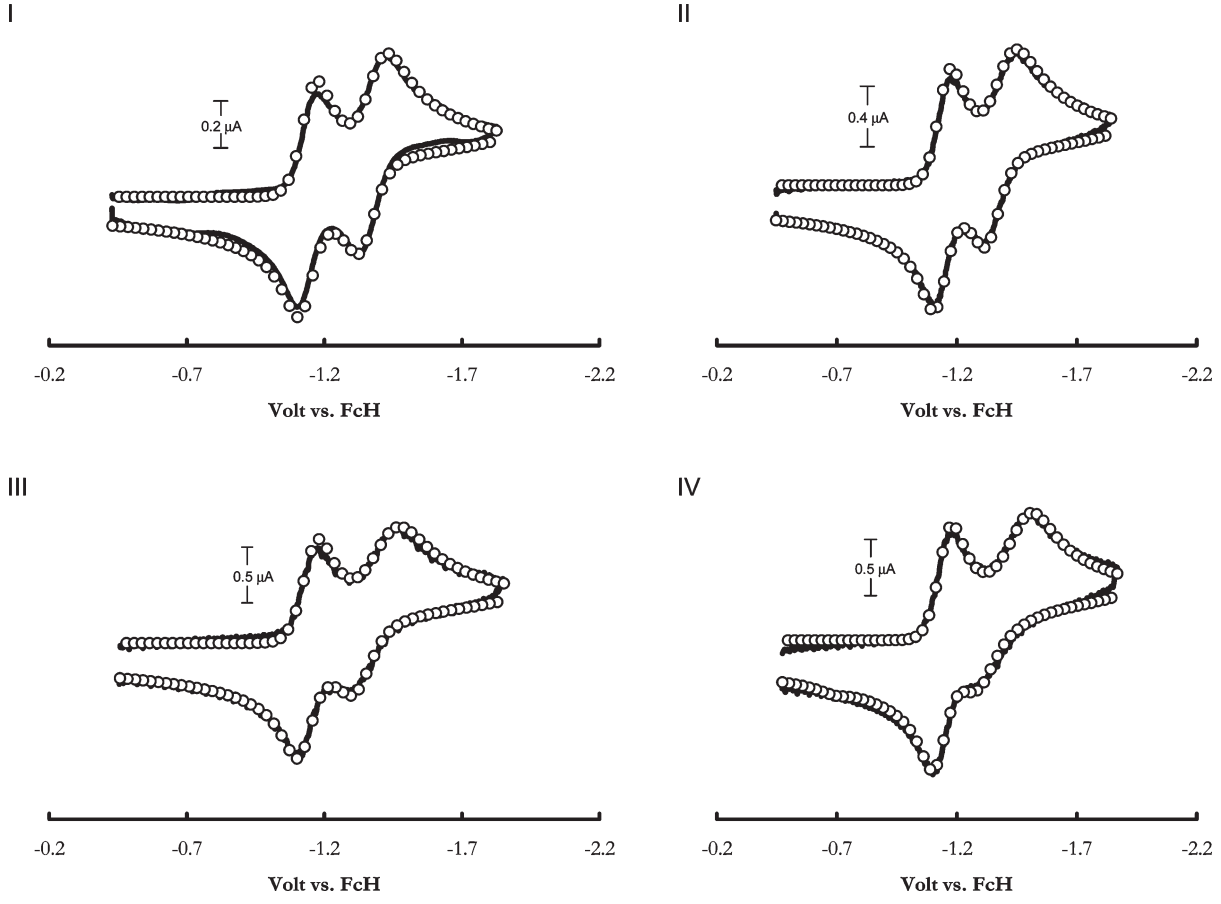

Figure 7. Simulation of $\mathbf{1}^-$ in THF under varying supporting electrolyte concentrations. (I) 8 mM [NBu_4][TFAB], 0.2 V/s, (II) 19 mM [NBu_4][TFAB], 0.5 V/s, (III) 38 mM [NBu_4][TFAB], 0.75 V/s, (IV) 75 mM [NBu_4][TFAB], 1 V/s. Circles represent simulated voltammograms and solid lines represent experimental data.

Table 4. Relevant Simulation Parameters for 0.28 mM $\mathbf{1}^-$ in THF Having Concentrations of [NBu_4][$B(C_6F_5)_4$] Varying from 8 mM to 75 mM[a]

Rxn or Symbol	8 mM	19 mM	38 mM	75 mM	Avg[b]
$E_{1/2}^{2,3}$	−1.353	−1.380	−1.379	−1.382	−1.361 ± 0.001
α	0.34	0.33	0.36	0.43	0.33 ± 0.01
k_s (cm s^{-1})	0.0024	0.0028	0.0022	0.0016	0.0026 ± 0.0001
K_3 (M^{-1})[c]	2.04	3.78	2.91	3.31	4.09 ± 0.34
k_f (M^{-1} s^{-1})[c]	92.2	50.8	84.7	120	273 ± 60

[a] CV scans were recorded at 2 mm gce. Only values for the square scheme of Scheme 2 are listed. Those used for the $\mathbf{1}^{1-/2-}$ couple were $E_{1/2}^{1,2}$ = −1.14 V, α = 0.50, k_s = 1 cm s^{-1}. Potentials vs ferrocene. [b] Average of entire group of simulations under all 24 sets of scan rate and concentration conditions. [c] See reference 34.

process, especially in light of the tetrahedral structure reported for the aforementioned $[Ag(mnt)_2]^{3-}$.[37] The separation of $E_{1/2}$ values for these reactions (0.22 V in THF) is much smaller than observed with other square-planar metal dithiolate complexes. For example, the $\Delta E_{1/2}$ values for other comparable late-metal $[M(mnt)_2]^{-/2-/3-}$ processes are 1.90, 2.33, and 2.63 V for Ni, Pd, and Pt, respectively,[14] and 1.07 V for Cu.[12] Structural reorganization of the gold-mnt trianion may be an important source of its thermodynamic stabilization.

As well established by the extensive medium effects observed in these investigations, the initially formed trianion, $[Au(mnt)_2]^{3-}$, interacts strongly with a number of solvents, so that the overall electrochemical reaction for the reduction of

Table 5. Energies of Nitrile Bands in IR Spectra of $[Au(mnt)_2]^{z-}$ in Various Matrixes

matrix	$[Au(mnt)_2]^-$	$[Au(mnt)_2]^{2-}$	$[Au(mnt)_2]^{3-}$
dichloromethane[a]	2213, 2226 cm^{-1}	2195 cm^{-1}	2183 cm^{-1}
THF[b]	2210, 2222 cm^{-1}	2193 cm^{-1}	2184, 2190 cm^{-1}
KBr	2210, 2223 cm^{-1}	2191 cm^{-1}	2181, 2188 cm^{-1}

[a] Solvent contained 0.1 M [NBu_4][BF_4]; data from reference 12. [b] Solvent contained 0.1 M [NBu_4][PF_6]; data from present work.

$\mathbf{1}^{2-}$ may be expressed as eq 7. This formulation indicates that one-electron reduction of $[Au(mnt)_2]^{2-}$ includes

$$[Au(mnt)_2]^{2-} + e^- + Solv + C^+ \rightleftharpoons [CAu(mnt)_2 \cdot Solv]^{2-} \quad (7)$$

uptake of one or more equiv of solvent and an additional tightly ion-paired electrolyte cation. Equation 7 essentially describes the cross-reaction in the square scheme section of Scheme 2. Implicit is the fact that both the solvent and the C^+ interact in their usual ways with the dianion $[Au(mnt)_2]^{2-}$. The voltammetry shows definitively that the "medium rich" reduced product, $[CAu(mnt)_2 \cdot Solv]^{2-}$, is favored in solvents such as acetonitrile and dichloromethane and is reoxidized at a potential, $E_{1/2}^{S2,3}$, positive of that of the "desolvated" trianion, which occurs at $E_{1/2}^{2,3}$. In a weakly solvating medium with low electrolyte concentrations, there is a more

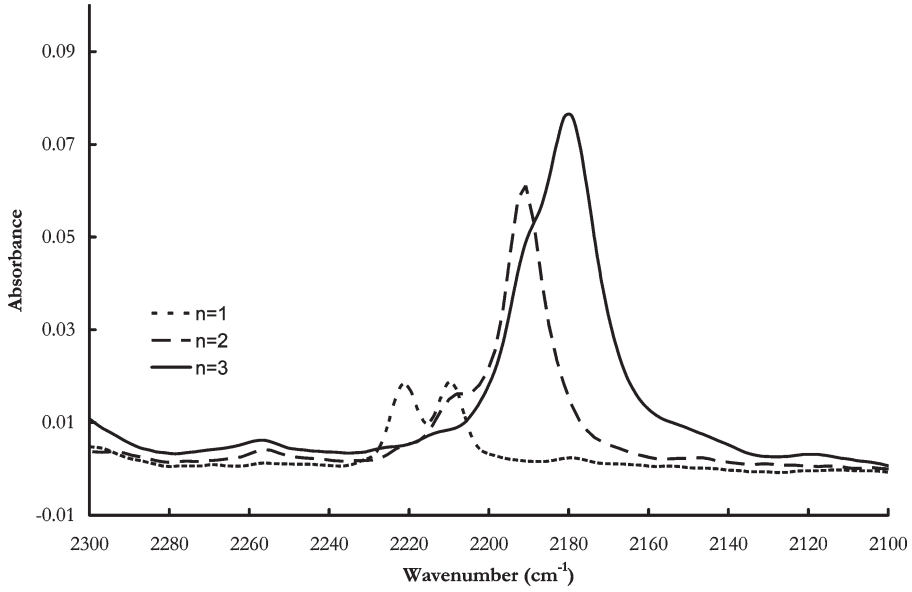

Figure 8. IR spectroelectrochemistry of 1^{n-} (n indicated in legend) in 0.1 M $[NBu_4][PF_6]$/THF.

Table 6. Wavelengths of Visible and near IR Absorptions Observed for $\mathbf{1}^{n-}$ (n = 1, 2, 3)[a]

$\mathbf{1}^{-}$	1^{2-}	1^{3-}
1020 nm (50)	1020 nm (250)	1020 nm (120)
970 (35)	970 (200)	970 (90)
745 (50)	720 (430)	
475 (120)	590 (240)	

[a] Numbers in parentheses are molar extinction coefficients in $M^{-1}\,cm^{-1}$.

competitive equilibrium between $[Au(mnt)_2]^{3-}$ and $[CAu(mnt)_2\cdot Solv]^{2-}$ that is responsible for the CV behavior observed in THF.

Whereas the existence of the solvento complexes is well established by these data, the precise nature of the intermolecular solvent−solute interactions is more obscure. Specific solvation of molecules by acetonitrile or dichloromethane generally relies on the Lewis base character of the solvents.[38] Not only are Lewis-acidic centers absent in $\mathbf{1}^{3-}$, but there is also no indication that either of these solvents interacts strongly with the other identically charged, square-planar, metal complexes $[M(mnt)_2]^{3-}$ (M = Co,[6d,e] Rh,[6d,e] Ni,[14] Cu[12,39]). Furthermore, the tetrahedral or quasi-tetrahedral structure assumed[40,41] for $\mathbf{1}^{3-}$ also mitigates against any tendency toward 5-coordination of the metal center. Rather, it is the unique *electronic structure* of the fully reduced gold complex that is likely to account for its unusual solvent interactions. Whereas the highest occupied molecular orbitals (HOMOs) of the Co, Ni, and Cu-based trianions have significant, if not dominant, metal character, the HOMO of $[Au(mnt)_2]^{3-}$ is more highly located on the ligands. If one assumes that the metal−ligand charge distribution does not change greatly in the square-planar to tetrahedral rearrangement of $[Au(mnt)_2]^{3-}$, as much as 80% of the charge will be localized on the four sulfur atoms, making them highly nucleophilic. Consequently, the sulfur atoms may interact strongly with a solvent capable of hydrogen-bonding. This kind of interaction is well-known for the strong accepting solvents dichloromethane and acetonitrile (see structures below)[42]

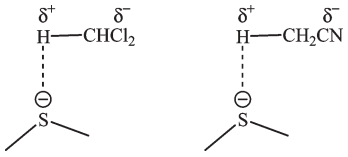

and is likely to be responsible for the $[Au(mnt)_2\cdot Solv]^{3-}$ complexes formed in those solvents. The weak medium-based complex observed in THF is unlikely to have such a structure for, to our knowledge, hydrogen-bonding to the H atoms of the strong donor solvent THF is unknown. Both the electrolyte cation and the solvent appear to play a role in the medium complex in THF, and calculations are likely to be necessary to describe the specific nature and energies of the medium interactions in donor solvents.

Conclusion

Cathodic ET reactions of mnt complexes of the later transition metals have been shown previously to be highly reversible (quasi-Nernstian) processes, with well-separated $E_{1/2}$ values. The most glaring exception to this generality was that of the reduction of $[Au(mnt)_2]^{-}$, which forms the corresponding trianion in consecutive closely spaced

(38) See, for example: (acetonitrile) (a) Chase, P. A.; Romero, P. E.; Piers, W. E.; Parvez, M.; Patrick, B. O. *Can. J. Chem.* **2005**, *83*, 2098; (dichloromethane):(b) Park, Y.-D.; Kim, J.-J.; Cho, S.-D.; Lee, S.-G.; Falck, J. R.; Yoon, Y.-J. *Synthesis* **2005**, 1136.

(39) The one-electron reduction of $[Cu(mnt)_2]^{2-}$ is quasi-Nernstian in both dichloromethane and acetonitrile containing 0.1 M $[NBu_4][PF_6]$ when the voltammetry is carried out at a glassy carbon electrode. Some irreversibility and electrode history is observed when a platinum or gold working electrode is employed (A. Bijunas, unpublished work at the University of Vermont).

(40) Five-coordinate Au(I) complexes are rare. See: Gimeno, M. C.; Laguna, A. *Chem. Rev.* **1997**, *97*, 511.

(41) Yam, V.W-W.; Chan, C.-L.; Choi, S.W-K.; Wong, K.M-C.; Cheng, E.C-C.; Yu, S.-C.; Ng, P.-K.; Chan, W.-K.; Cheung, K.-K. *Chem. Commun.* **2000**, 53.

(42) (a) Kamlet, M. J.; Taft, R. W. *J. Chem. Soc., Perkin Trans. II* **1979**, 337. (b) Novoa, J. J.; Whangbo, M.-H. *J. Am. Chem. Soc.* **1991**, *113*, 9017. (c) Cerda, J. F.; Koder, R. L.; Lichtenstein, B. R.; Moser, C. M.; Miller, A.-F.; Dutton, P. L. *Org. Biomol. Chem.* **2008**, *6*, 2204.

one-electron processes, the second of which is electrochemically irreversible. The present work shows that the reduction of $[Au(mnt)_2]^{2-}$ to $[Au(mnt)_2]^{3-}$ proceeds by a EC mechanism in which the heterogeneous ET step is slow owing to structural rearrangement of the AuS_4 geometry, and the chemical reaction involves the trianion $[Au(mnt)_2]^{3-}$ with the solvent and electrolyte medium. Strong solvento-complexes which are formed rapidly in acetonitrile and dichloromethane are quantitatively reoxidized back to the original "medium-free" square-planar dianionic gold complex by a CE mechanism. Of the five solvents studied (acetonitrile, dichloromethane, DMF, DMSO, and THF), all but THF form strong complexes with $[Au(mnt)_2]^{3-}$ that can be observed by cyclic voltammetry. Identically charged square-planar mnt complexes of Co, Ni, and Cu show no evidence of specific solvation under similar medium conditions, leaving the molecular or electronic structure of the gold complex as the source of its different behavior. Interaction of the solvent with the uniquely highly charged sulfur atoms of $[Au(mnt)_2]^{3-}$, probably through an H-bonding interaction, is most likely responsible for the observed complex/solvent interactions.

Acknowledgment. We thank the National Science Foundation for support under NSF CHE-0411703 and -0808909. We also acknowledge the preliminary work done on this system by Al B. Bijunas at the University of Vermont.

Supporting Information Available: Seven figures including chronoamperometry and chronocoulometry of $\mathbf{1}^-$, LSV scans obtained in bulk electrolyses, CV scans of $\mathbf{1}^-$ in the presence of $[Na(2.2.2)]^+$, a set of 16 CV simulations of $\mathbf{1}^-$ in THF, and UV−vis spectra. This material is available free of charge via the Internet at http://pubs.acs.org.